nature structural & molecular biology

Article

https://doi.org/10.1038/s41594-022-00850-3

# AAA+ protease-adaptor structures reveal altered conformations and ring specialization

In the format provided by the authors and unedited

## SUPPLEMENTARY INFORMATION

**Supplementary Table 1.** Oligonucleotides used in this study.

| Oligonucleotide Name | Purpose | Oligonucleotide Sequence (5′ to 3′) |
|---|---|---|
| D1 pore-2 QTQ For | Round-the-horn mutagenesis of $^{QTQ}$ClpA | CAAGGTGGTCAGGTCGATGCG |
| D1 pore-2 QTQ Rev | Round-the-horn mutagenesis of $^{QTQ}$ClpA | AGTCTGACCCGCACCGATAATGG |
| D1 pore-2 G For | Round-the-horn mutagenesis of $^{GGG}$ClpA | GGAGGTGGTCAGGTCGATGCG |
| D1 pore-2 GG Rev | Round-the-horn mutagenesis of $^{GGG}$ClpA | GCCTCCACCCGCACCGATAATGG |
| D1 pore-2 298 For | Round-the-horn mutagenesis of $^{\Delta 295\text{-}297}$ClpA and $^{KYR}$ClpA | GGTGGTCAGGTCGATGCG |
| D1 pore-2 294 Rev | Round-the-horn mutagenesis of $^{\Delta 295\text{-}297}$ClpA | ACCCGCACCGATAATGG |
| D1 pore-2 KYR Rev | Round-the-horn mutagenesis of $^{KYR}$ClpA | ACGATATTTACCCGCACCGATAATGG |

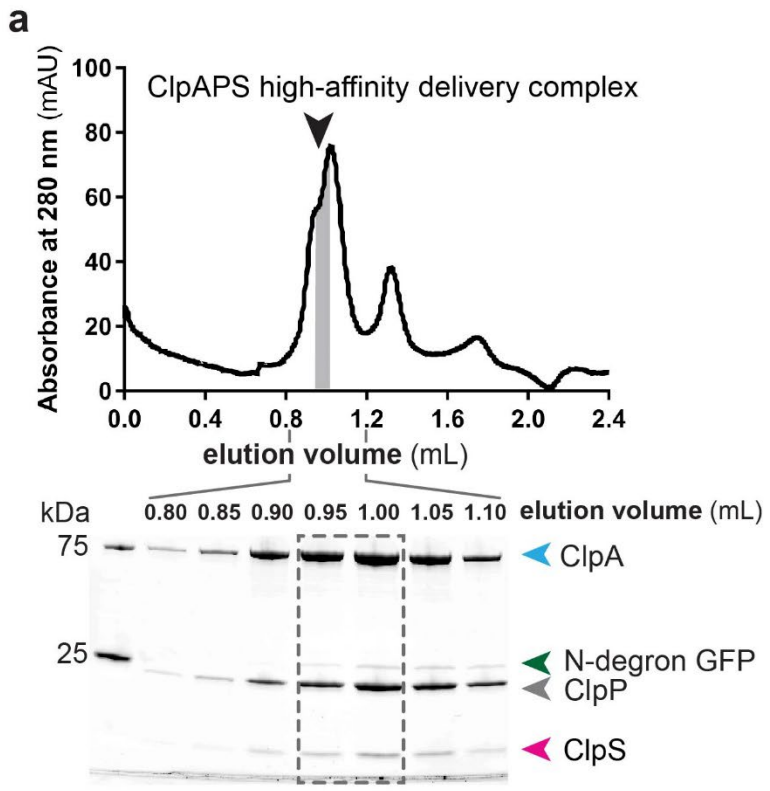


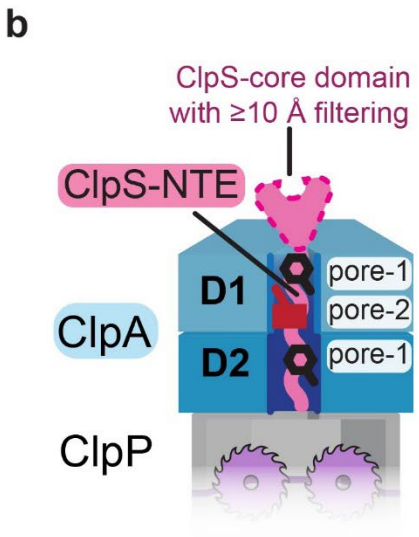


**Supplementary Figure 1. Overview of ClpAPS cryo-EM structural features.**
**a**, Size-exclusion chromatography (top panel) of a complex of ClpA, ClpP, ClpS, and YLFVQELA-GFP (an N-degron substrate) assayed by SDS-PAGE (bottom panel). Gray shaded area and boxed area indicate the fractions pooled for cryo-EM. Preparation of ClpAPS•YLFVQELA-GFP complexes by SEC was performed independently five times (during initial grid screening and optimization); only the shown SEC-purified sample was used to prepare the single grid imaged for data collection. Uncropped gel image at the end of the SI file. **b**, Cartoon of pore loops that interact with the ClpS NTE and proteins resolved in cryo-EM structures.

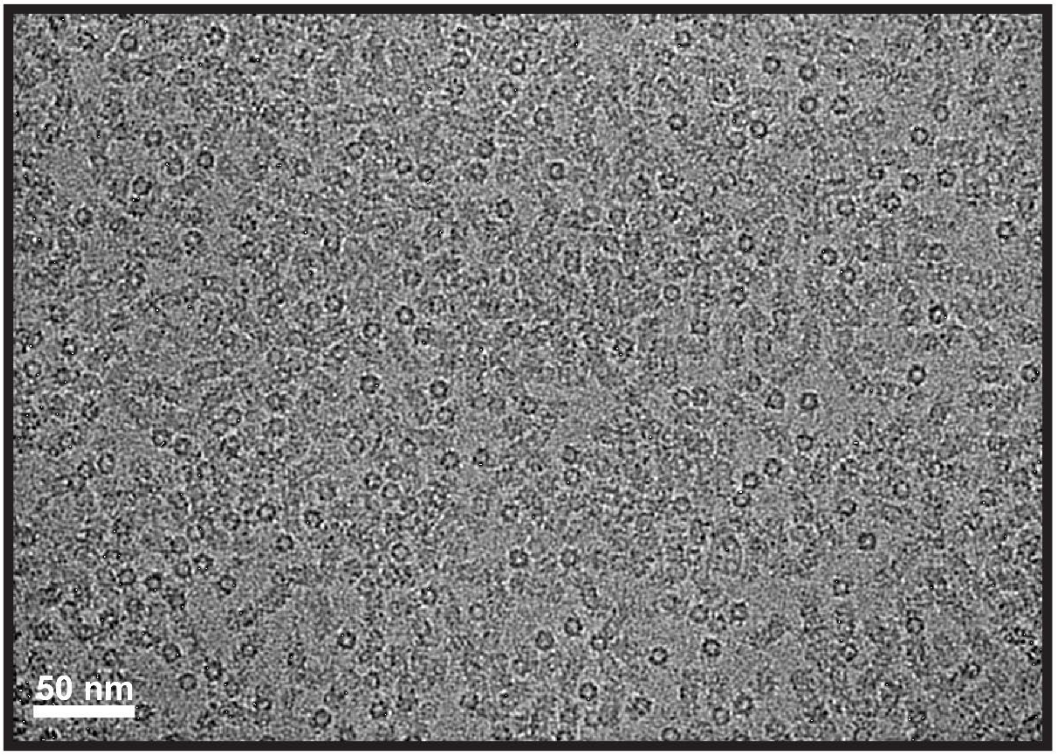


**Supplementary Figure 2. ClpAPS cryo-EM micrograph.**
Representative cryo-EM micrograph of ClpAPS•N-degron GFP complexes from cryo-EM data collection (9,169 micrographs collected total). The scale bar corresponds to 50 nm. The majority of particles are doubly capped with two $ClpA_6$ molecules per $ClpP_{14}$.

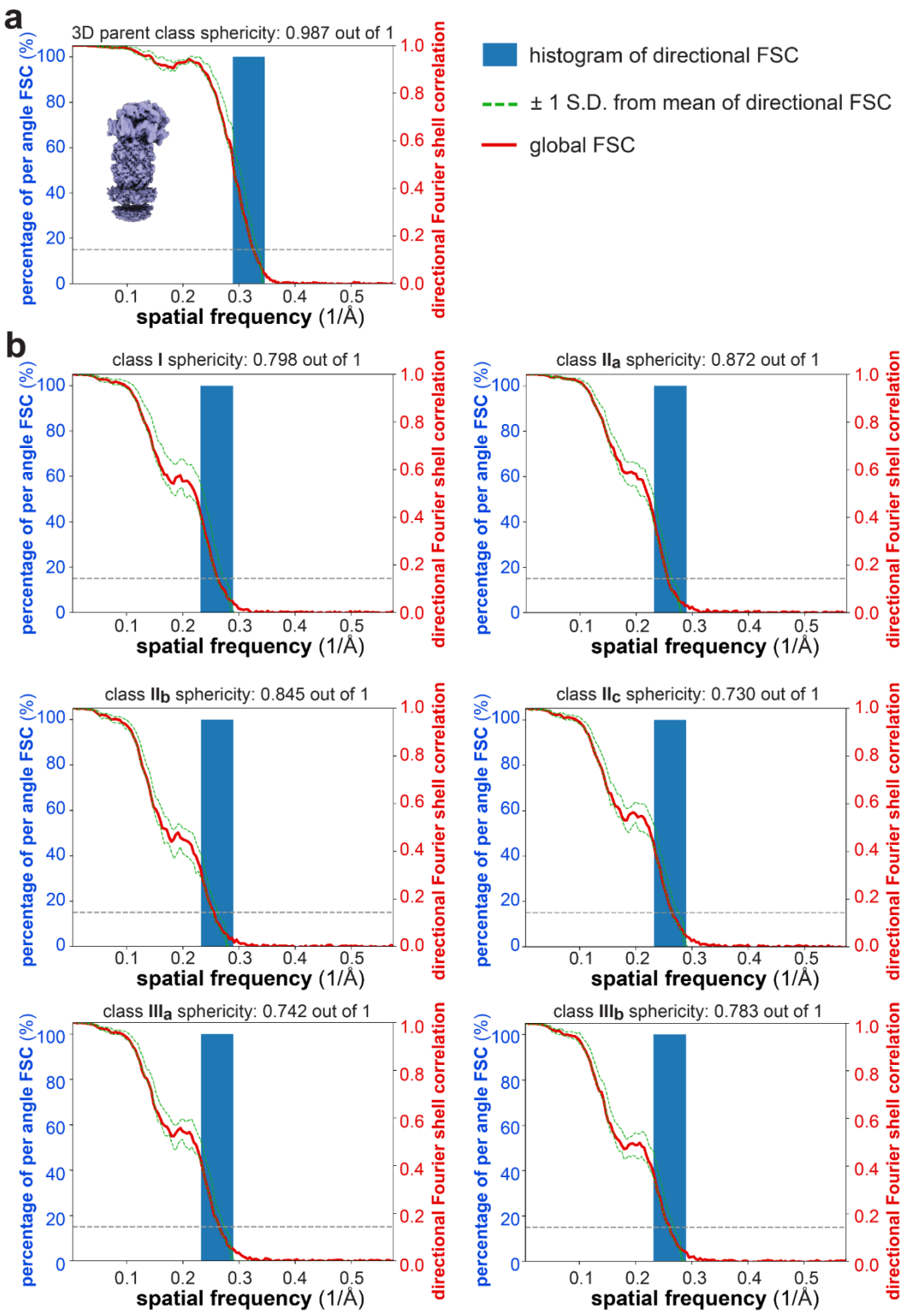


**Supplementary Figure 3. 3DFSC sphericity**

3DFSC plots of classes **I**, **II**, and **III** and parent class prior to focused classification. Due to non-uniform box dimensions following density modification, intermediate maps from RELION-3 (from 3D auto-refine) were used as 3DFSC inputs for class **I**, **II**, and **III** structures.

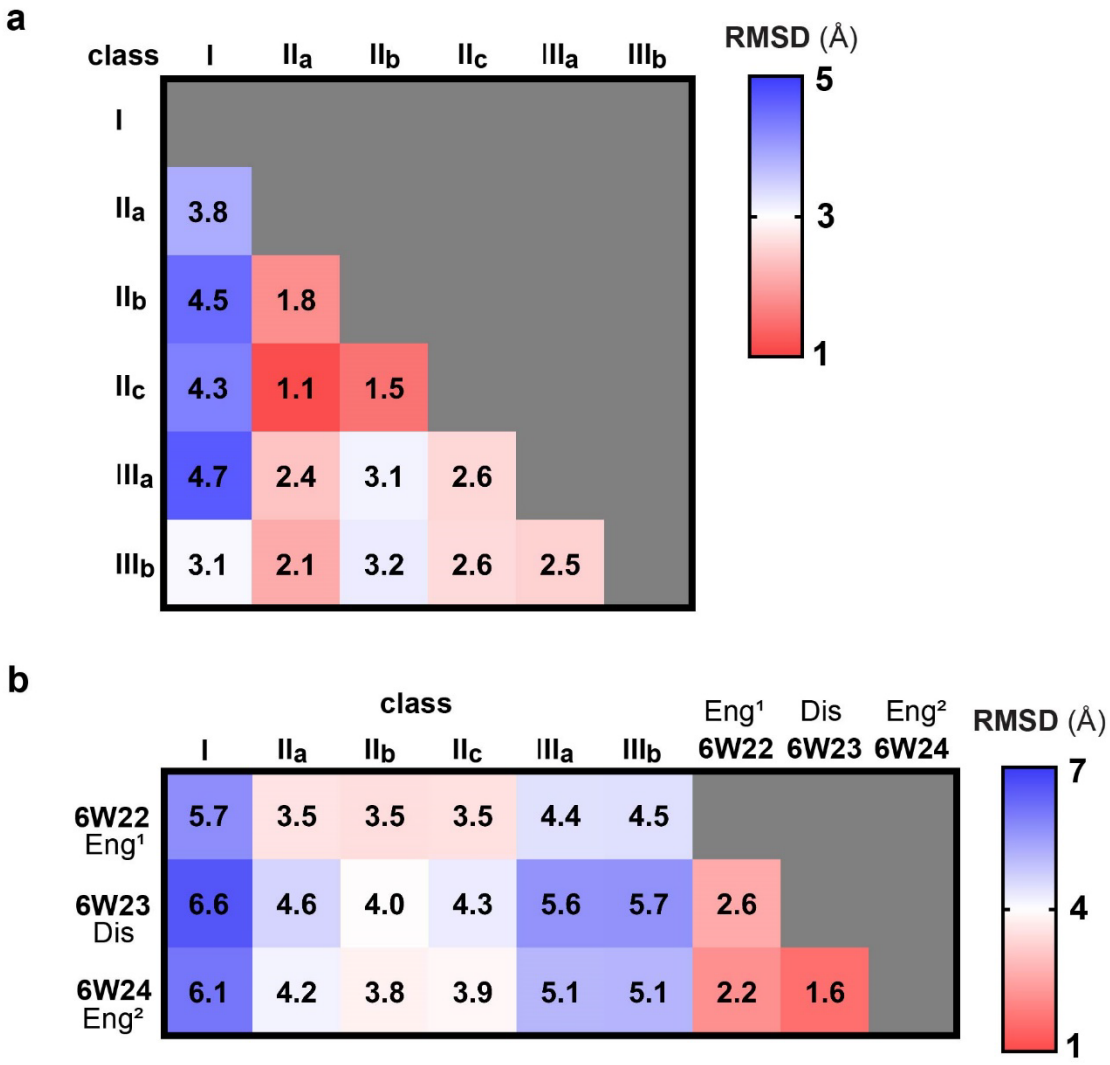


**Supplementary Figure 4. Cα RMSD analysis of ClpAP structures.**
**a**, Pairwise RMSD (Å) calculations of class **I**, **II**, and **III** subclasses between ClpA Cα atoms in subunits A through F using PyMOL "align". **b**, Pairwise RMSD comparisons of ClpA Cα atoms in ClpAPS cryo-EM structures and ClpAP•RepA-GFP structures (PDB 6W22, 6W23, and 6W24), using PyMOL "align".

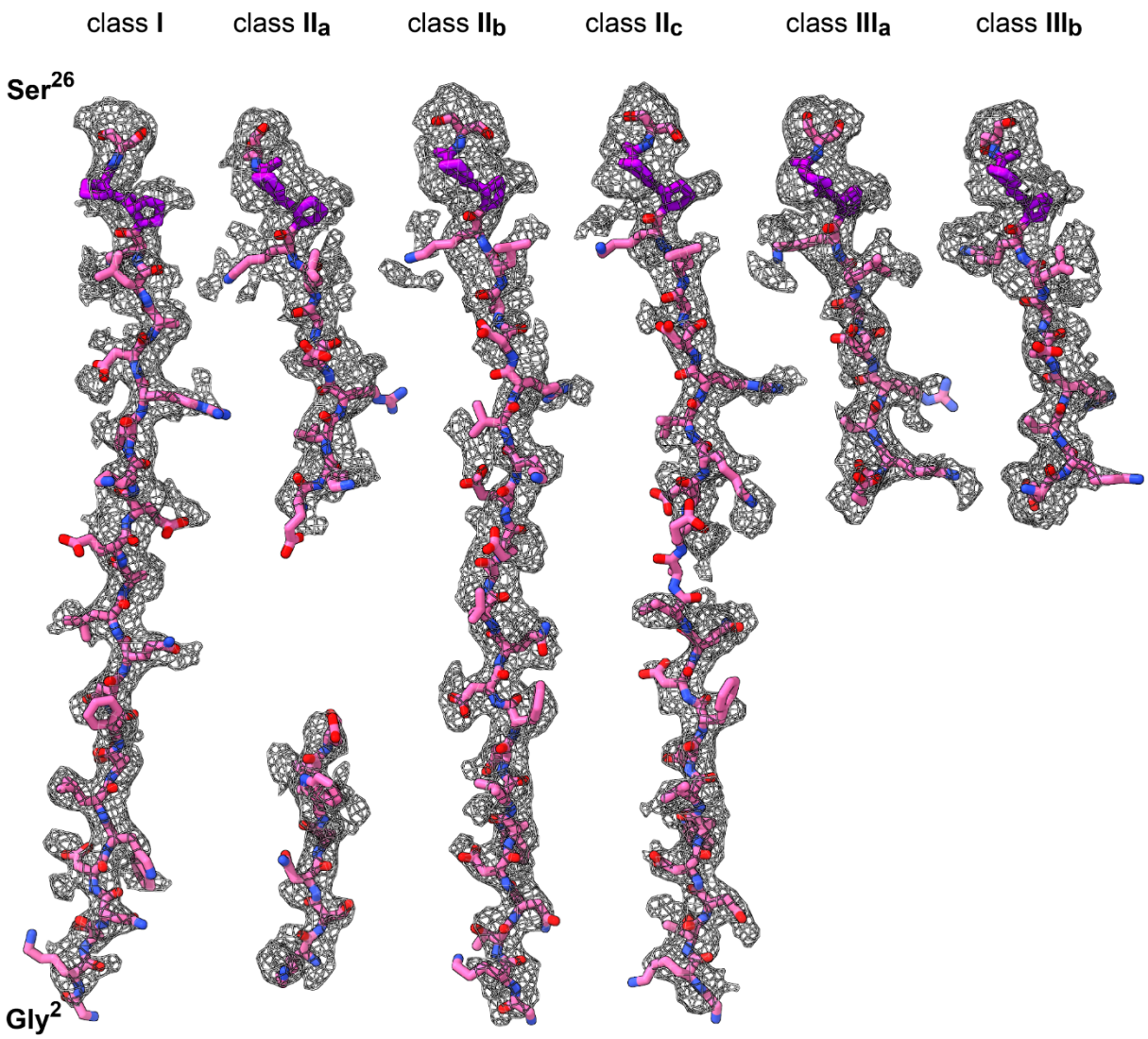


**Supplementary Figure 5. ClpS NTE map–model comparisons.**
ClpS NTE density (mesh at contour level 0.25) and atomic models (shown in sticks) in the ClpA axial channel in classes **I**, **II**, and **III**. The junction sequence residues, $Pro^{24}$ and $Pro^{25}$, are colored purple, whereas the rest of the NTE is colored pink.

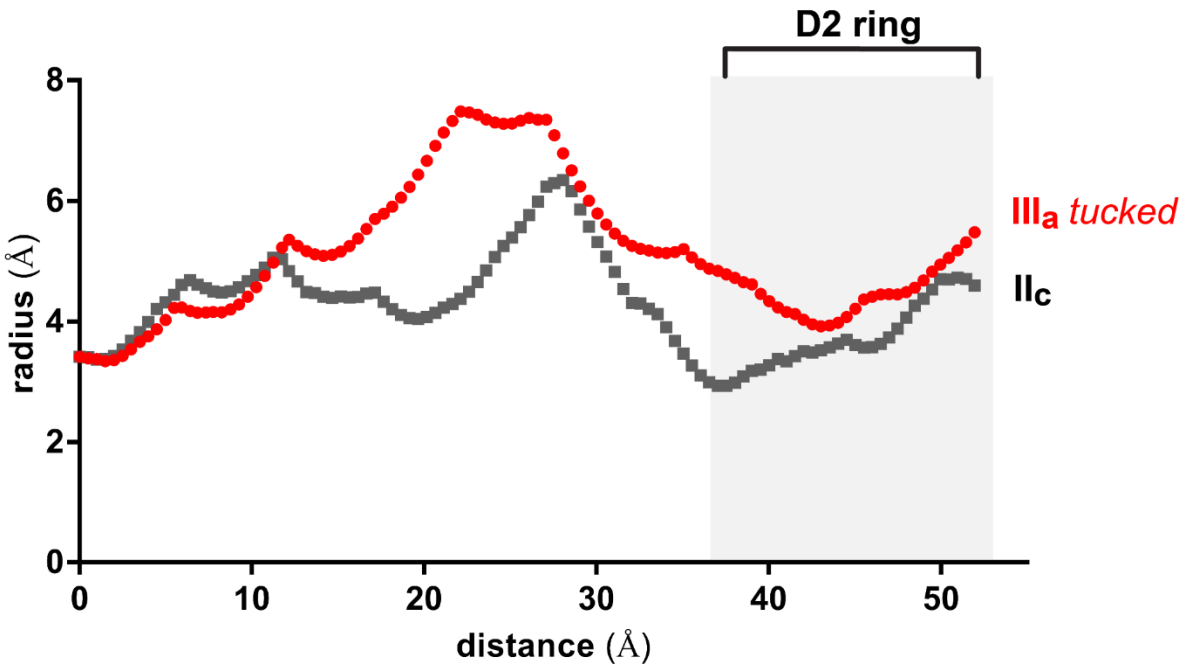


**Supplementary Figure 6. Axial channel radius comparison.** Plot of channel radius vs. channel distance (length of channel from top to bottom of ClpA) calculated by CAVER[1] in class-**II$_c$** (dark gray squares) and class-**III$_a$** (red circles) atomic models. Portion of axial channel in D2 ring is indicated by the light gray box.

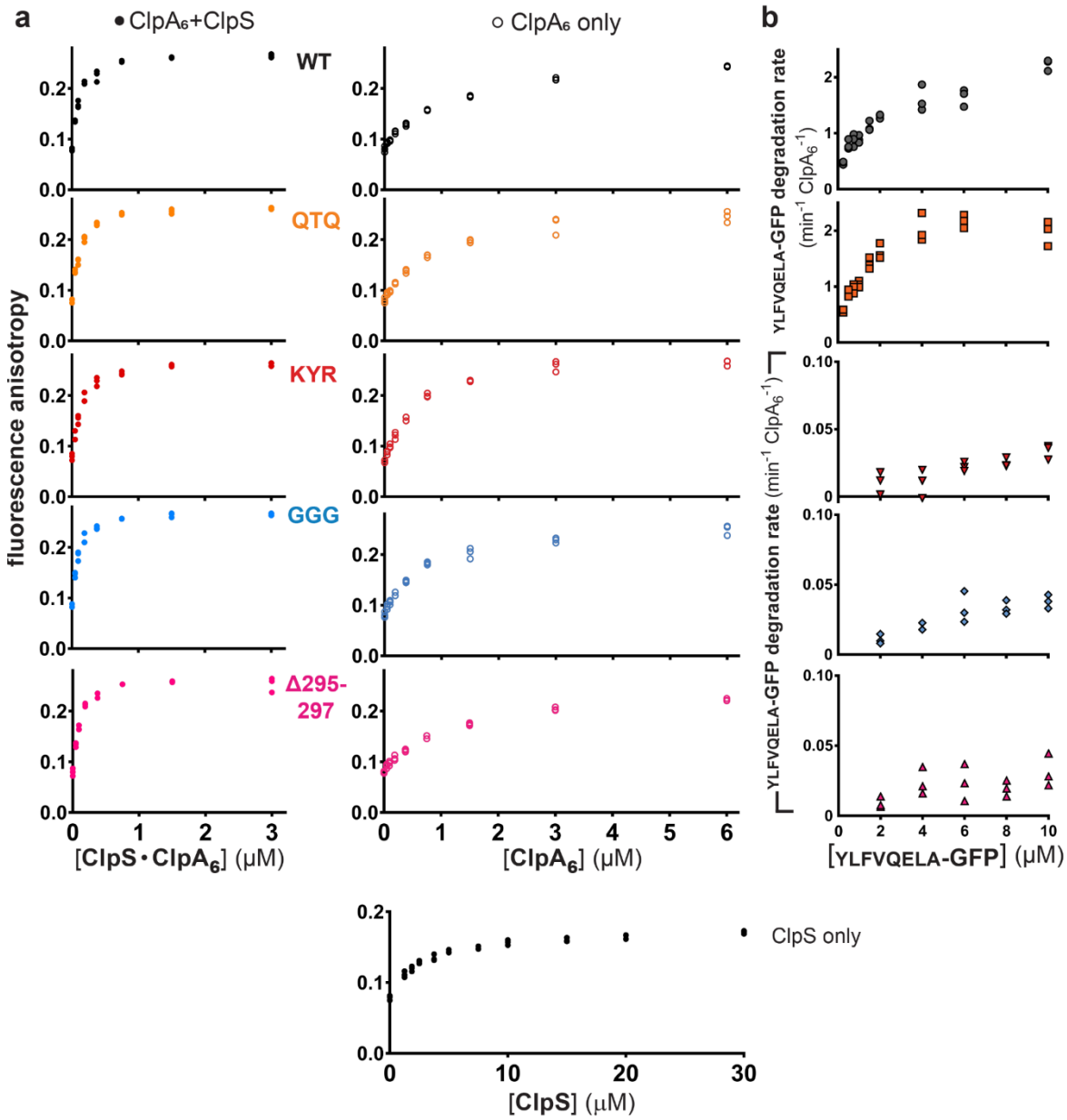


**Supplementary Figure 7. Individual fluorescence anisotropy and YLFVQELA-GFP degradation rate values from Fig. 5a–b. a**, Fluorescence anisotropy of ClpA pore-2 variants alone ($ClpA_6$, open circles), with an equimolar mixture with ClpS (+ClpS, filled circles), or ClpS only (bottom right panel), titrated in increasing concentrations against a fixed concentration of fluorescein-labeled N-degron peptide. **b**, Kinetic analysis of YLFVQELA-GFP degradation by ClpA D1 pore-2 variants (see *Methods* for concentrations). The graphed y-axis of WT and the KYR variant ranges from 0–2.5 $min^{-1}$ $ClpA_6^{-1}$, whereas the y-axis shown for KYR, GGG, and Δ295–297 variants ranges from 0–0.10 $min^{-1}$ $ClpA_6^{-1}$.

## SUPPLEMENTARY REFERENCES

1. Jurcik, A., Bednar, D., Byska, J., Marques, S. M., Furmanova, K., Daniel, L., Kokkonen, P., Brezovsky, J., Strnad, O., Stourac, J., Pavelka, A., Manak, M., Damborsky, J., & Kozlikova, B. CAVER Analyst 2.0: analysis and visualization of channels and tunnels in protein structures and molecular dynamics trajectories. Bioinformatics (Oxford, England), 34(20), 3586–3588 (2018).

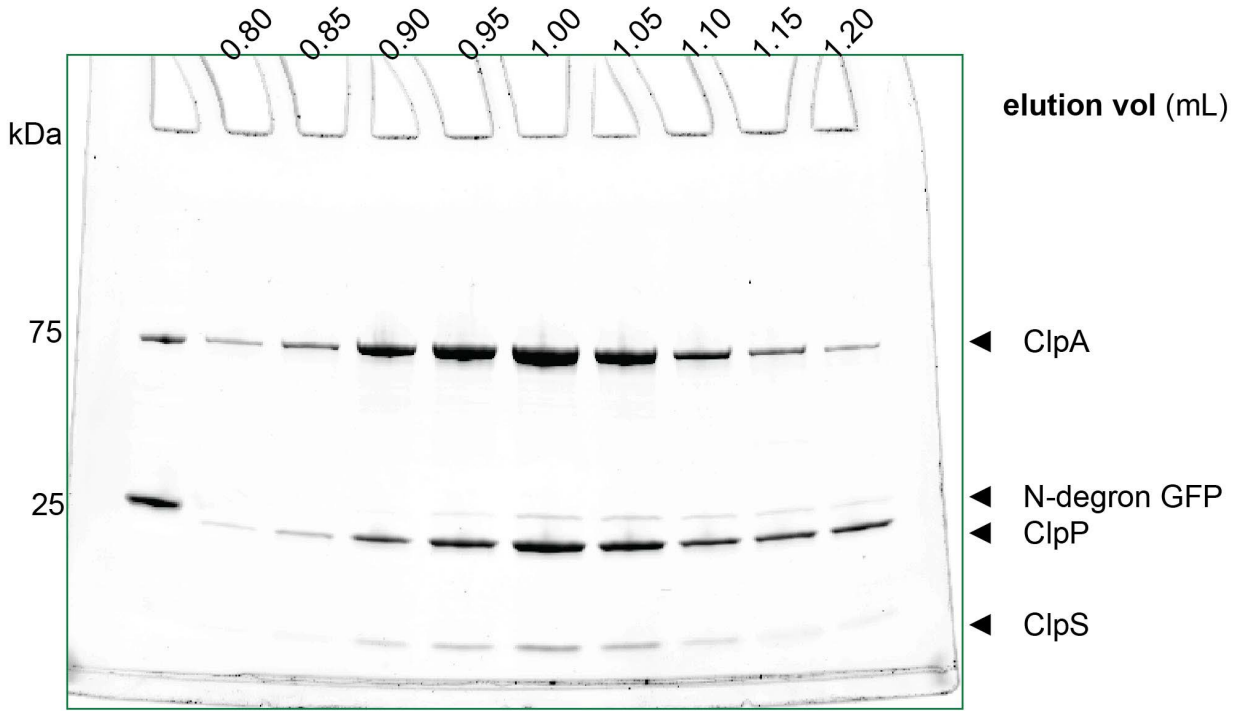


**Unprocessed gel image for Supplementary Fig. 1a**. SDS-PAGE gel (stained with SYPRO Red) of ClpAPS•YLFVQELA-GFP complexes prepared by SEC.